

Motion Control based on Disturbance Estimation and Time-Varying Gain for Robotic Manipulators

Xinyu Jia, Jun Yang, Kaixin Lu and Haoyong Yu, *Senior Member, IEEE*

Abstract—To achieve high-accuracy manipulation in the presence of unknown dynamics and external disturbance, we propose an efficient and robust motion controller (named TvUDE) for robotic manipulators. The controller incorporates a disturbance estimation mechanism that utilizes reformulated robot dynamics and filtering operations to obtain uncertainty and disturbance without requiring measurement of acceleration. Furthermore, we design a time-varying control input gain to enhance the control system’s robustness. Finally, we analyze the boundness of the control signal and the stability of the closed-loop system, and conduct a set of experiments on a six-DOF robotic manipulator. The experimental results verify the effectiveness of TvUDE in handling internal uncertainty and external static or transient disturbance.

I. INTRODUCTION

Robotic manipulators are gradually replacing humans in performing repetitive, monotonous, or hazardous tasks [1]. The quality of manipulation largely depends on the motion control performance. In general, dynamics-based motion tracking control allows the robot to behave more precisely than using kinematics alone, since the former can take into account more physical properties of the robot or the environment [3]. However, the robot dynamics in the real world is too complex to be modelled exactly, such as friction or other non-smooth dynamics [2]. The external force (load, collision or human-robot interaction) can also affect tracking accuracy. Therefore, the effect induced by these internal uncertainty and external disturbance should be addressed to achieve precise motion control.

Many control strategies have been developed to compensate for uncertainty and disturbance. The proportional-integral-derivative (PID) control with dynamics as feedforward compensation is popular in industrial manipulators [3]. The actual link inertia or joint friction is often obtained through system model identification [4]. However, the identified result is rough and easily mismatched from the true model. The learning method can also construct the unknown dynamics, but it will bring heavy computation burden and the parameter tuning is not trivial in general [5]. Recently, observer-based control schemes have shown huge potential in solving uncertainty and disturbance to improve control accuracy [6]. For example, in [7], the disturbance torque of a linear motor system is estimated by the disturbance observer (DOB). The nonlinear disturbance observer (NDO)

This work was supported by the Science and Engineering Research Council, Agency of Science, Technology and Research, Singapore, under the National Robotics Program, with A*star SERC Grant No.192 25 00054.

Authors are with the Department of Biomedical Engineering, National University of Singapore, 117583, Singapore. (Email: bieyhy@nus.edu.sg)

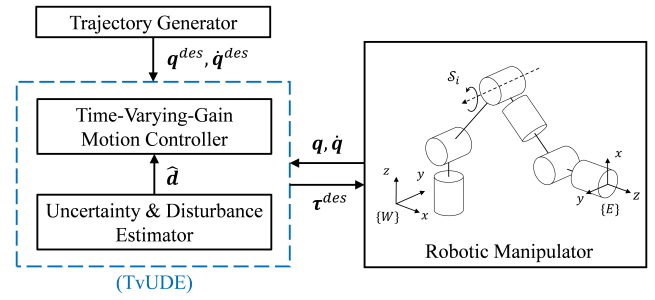


Fig. 1. The proposed motion control framework for robotic manipulators to handle uncertainty and disturbance in tracking tasks.

is also developed and applied on a robotic manipulator in [8]. However, both types of observer require to identify model information and construct extra filters. The extended state observer (ESO) presented in [9] is widely adopted in disturbance estimation, and some ESO-based methods are proposed as well, e.g., adaptive ESO [10] [11]. Nevertheless, implementing ESO on high-dimensional robots is relatively difficult due to its complicated parameter tuning process.

The unknown system dynamics estimator (USDE) in [12]–[14] is formulated on the basis of low pass filters with simple formulation but demonstrates impressive estimation performance of disturbance. However, the method is validated on a planar robot with only two degrees of freedom (DOF), instead of a general manipulator with six or more DOFs, of which dynamics are more nonlinear and coupled. Besides, there is no discussion in terms of different disturbance conditions, where the fixed control gain might make the robot fail to handle complex external disturbance in practice. In [15], the authors provide an idea of selecting control input gain by a project gradient estimator (PGE) [16] and verify it with the ESO on series elastic actuators (SEAs).

In this paper, a motion controller based on uncertainty and disturbance estimation and time-varying control gain (TvUDE) is proposed for robotic manipulators. The estimator without measurement of acceleration can obtain unknown dynamics and disturbance in real time, while the time-varying gain allows the robot to exhibit more robustness when meeting various external disturbance. The contributions of this work are: 1) we present an efficient and robust motion control framework for general manipulators; 2) we combine the disturbance estimation and the time-varying gain to handle various disturbance in tracking tasks; 3) we verify the proposed approach through a set of experiments on a six-DOF manipulator.

II. SYSTEM MODEL

The screw theory provides concise expression and efficient calculation in robot modelling, especially for high-dimensional rigid robots [17]. It does not require all parameters of the link coordinates as in conventional methods [3]. For a serial manipulator with n rotational DOFs, the forward kinematics (FK) is given by

$$\mathbf{T} = e^{[\mathcal{S}_1]\theta_1} e^{[\mathcal{S}_2]\theta_2} \dots e^{[\mathcal{S}_n]\theta_n} \mathbf{N} \quad (1)$$

where the transform matrix $\mathbf{T} \in SE(3)$ denotes the end-effector pose, $[\mathcal{S}_i]\theta_i \in se(3)$ is the exponential coordinate of the joint $i = 1, \dots, n$. $\mathbf{N} \in SE(3)$ is the end-effector pose when all joint angles are defined to zero as initial.

For the inverse kinematics (IK) solver, by formulating a quadratic programming problem with equality and inequality constraints as Eq. (2), all joint limitations are simultaneously considered. The resulted trajectory is smoother than that of common numerical IK which simply clamps the result after obtaining joint velocity [17].

$$\begin{aligned} \min_{\dot{\mathbf{q}}} \quad & \| \mathbf{J}\dot{\mathbf{q}} - \mathbf{V}^{des} \|^2 + \lambda^2 \|\dot{\mathbf{q}}\|^2 \\ \text{s.t.} \quad & \left\{ \begin{array}{l} \dot{\mathbf{q}}_{min} \leq \dot{\mathbf{q}} \leq \dot{\mathbf{q}}_{max} \\ \mathbf{q}_{min} \leq \mathbf{q} \leq \mathbf{q}_{max} \\ \mathbf{q} = \mathbf{q} + \dot{\mathbf{q}}\Delta t \end{array} \right. \end{aligned} \quad (2)$$

The first term in Eq. (2) is to minimize the error between $\mathbf{J}\dot{\mathbf{q}}$ and the designed twist $\mathbf{V}^{des} = (\boldsymbol{\omega}^{des}, \mathbf{v}^{des}) \in \mathbb{R}^6$, where $\boldsymbol{\omega} \in \mathbb{R}^3, \mathbf{v} \in \mathbb{R}^3$ denote the angular velocity and linear velocity of the end-effector, respectively. The mapping between the transform matrix and the twist is $\dot{\mathbf{T}}\mathbf{T}^{-1} = [\mathbf{V}] \in se(3)$. The second term is to avoid singularity with a damping coefficient λ . $\mathbf{q} \in \mathbb{R}^n$ is the vector of joint position with the lower bound \mathbf{q}_{min} and the upper bound \mathbf{q}_{max} . Δt is the time step of control loop.

Similarly, adopting screw concept in recursive Newton-Euler algorithm (RNEA) can increase efficiency in computing dynamics or equation of motion as Eq. (3), compared with the energy-based Lagrangian method.

$$\mathbf{M}(\mathbf{q})\ddot{\mathbf{q}} + \mathbf{C}(\mathbf{q}, \dot{\mathbf{q}})\dot{\mathbf{q}} + \mathbf{g}(\mathbf{q}) = \boldsymbol{\tau} + \boldsymbol{\tau}_e \quad (3)$$

where $\mathbf{M} \in \mathbb{R}^{n \times n}, \mathbf{C} \in \mathbb{R}^{n \times n}, \mathbf{g} \in \mathbb{R}^n$ are the inertia matrix, the Coriolis and centrifugal matrix, and the gravity vector, respectively. $\boldsymbol{\tau} \in \mathbb{R}^n$ is the vector of joint torque and $\boldsymbol{\tau}_e \in \mathbb{R}^n$ is the vector of torque that external force generates on the robot, including friction, load, and etc.

III. ESTIMATION AND CONTROL

The control framework proposed is versatile to open chain robotic manipulators with torque-controlled hinge joints, as illustrated in Fig. 1. We first reformulate the dynamic model to avoid directly using acceleration signals, and then estimate uncertainty and external disturbance via observers. The estimated result is then used for the motion controller design, of which the control gain is time-varying that allows the manipulator to adapt to complex disturbance.

A. Dynamic Model Reformulation

Before designing estimators and controllers, we will reformulate the dynamic model as follows. First, the model obtained from CAD data might be inaccurate in practice due to manufacture error, and the friction or other non-smooth dynamics involved are too complex to be exactly modelled. Considering these uncertainties, the actual dynamics is

$$(\mathbf{M} + \Delta\mathbf{M})\ddot{\mathbf{q}} + (\mathbf{C} + \Delta\mathbf{C})\dot{\mathbf{q}} + (\mathbf{g} + \Delta\mathbf{g}) = \boldsymbol{\tau} + \boldsymbol{\tau}_e \quad (4)$$

Hence, instead of identifying these uncertainties, we define a lumped disturbance $\mathbf{d} \in \mathbb{R}^n$ that consists of all kinds of uncertainty and disturbance together as

$$\mathbf{d} = \boldsymbol{\tau}_e - (\Delta\mathbf{M}\ddot{\mathbf{q}} + \Delta\mathbf{C}\dot{\mathbf{q}} + \Delta\mathbf{g}) \quad (5)$$

Secondly, directly measuring joint acceleration is relatively difficult in practice. Though differentiating the joint velocity with respect to time can obtain $\ddot{\mathbf{q}}$, it will also bring undesired noise. Hence, to avoid using $\ddot{\mathbf{q}}$, the following auxiliary items are given

$$\mathcal{P}(\mathbf{q}, \dot{\mathbf{q}}) = \mathbf{M}\dot{\mathbf{q}} \quad (6)$$

$$\mathcal{H}(\mathbf{q}, \dot{\mathbf{q}}) = -\mathbf{C}^T\dot{\mathbf{q}} + \mathbf{g} \quad (7)$$

where $\mathcal{P} \in \mathbb{R}^n, \mathcal{H} \in \mathbb{R}^n$.

As a result, Eq. (4) is redefined as

$$\dot{\mathcal{P}}(\mathbf{q}, \dot{\mathbf{q}}) + \mathcal{H}(\mathbf{q}, \dot{\mathbf{q}}) = \boldsymbol{\tau} + \mathbf{d} \quad (8)$$

where the skew symmetric property of \mathbf{M} (i.e., $\dot{\mathbf{M}} = \mathbf{C}^T + \mathbf{C}$ [17]) is leveraged to avoid differential of \mathbf{M} .

The reformulated model of Eq. (8) presents two distinct advantages compared to Eq. (3). First, it is unnecessary to excessively concern about the accuracy of the actual robot model, which might help us skip the parameter identification for joint friction or link inertia in robot development. Then, the acceleration of the joint angle is included in $\dot{\mathcal{P}}$. Accordingly, we can avoid using the acceleration signal if the differential of \mathcal{P} is not necessary in controller design.

B. UDE Design

Except for $\ddot{\mathbf{q}}$, the measurement of $\dot{\mathbf{q}}$ and \mathbf{q} is generally available for a manipulator. With the known \mathbf{M}, \mathbf{C} and \mathbf{g} , the variables \mathcal{P} and \mathcal{H} can be calculated via Eq. (6) and Eq. (7). Hence, we formulate several filters as

$$\begin{cases} k\dot{\mathcal{P}}_f + \mathcal{P}_f = \mathcal{P} \\ k\dot{\mathcal{H}}_f + \mathcal{H}_f = \mathcal{H} \\ k\dot{\tau}_f + \tau_f = \boldsymbol{\tau} \end{cases} \quad (9)$$

where $k > 0$ is a filter coefficient, $\boldsymbol{\tau}$ is the last torque command. $\mathcal{P}_f, \mathcal{H}_f, \tau_f$ are the filtered variables set to zero at initial.

Then, applying filtering operations for both sides of Eq. (8) and replacing the differential term with Eq. (9), we have

$$\frac{\mathcal{P} - \mathcal{P}_f}{k} + \mathcal{H}_f = \boldsymbol{\tau}_f + \mathbf{d}_f \quad (10)$$

where $\hat{\mathbf{d}}_f$ is the filtered lumped disturbance. Finally, the UDE is given as

$$\hat{\mathbf{d}} = \mathbf{d}_f = \frac{\mathcal{P} - \mathcal{P}_f}{k} + \mathcal{H}_f - \boldsymbol{\tau}_f \quad (11)$$

With the help of filtering operations, the disturbance estimation effectively avoids the differential of variables. Before proving this estimator's convergence, we first give the following lemma.

Lemma 1. *The lumped disturbance \mathbf{d} of a robot system as Eq. (8) can be estimated via the UDE in Eq. (11), and the estimation error $\tilde{\mathbf{d}} = \mathbf{d} - \hat{\mathbf{d}}$ has the following property*

$$\dot{\tilde{\mathbf{d}}} = -\frac{1}{k}\tilde{\mathbf{d}} + \dot{\mathbf{d}} \quad (12)$$

Proof : Substituting the filter equations of Eq. (9) into the left hand side of Eq. (12), we have

$$\begin{aligned} \dot{\tilde{\mathbf{d}}} &= \dot{\mathbf{d}} - \dot{\hat{\mathbf{d}}} = \dot{\mathbf{d}} - \left(\frac{\dot{\mathcal{P}} - \dot{\mathcal{P}}_f}{k} + \dot{\mathcal{H}}_f - \dot{\boldsymbol{\tau}}_f \right) \\ &= \dot{\mathbf{d}} - \frac{1}{k}(\dot{\mathcal{P}} - \frac{\mathcal{P} - \mathcal{P}_f}{k} + \mathcal{H} - \mathcal{H}_f - \boldsymbol{\tau} + \boldsymbol{\tau}_f) \\ &= \dot{\mathbf{d}} - \frac{1}{k} \left[(\dot{\mathcal{P}} + \mathcal{H} - \boldsymbol{\tau}) - \left(\frac{\mathcal{P} - \mathcal{P}_f}{k} + \mathcal{H}_f - \boldsymbol{\tau}_f \right) \right] \\ &= -\frac{1}{k}\tilde{\mathbf{d}} + \dot{\mathbf{d}} \end{aligned} \quad (13)$$

The internal uncertainty or external disturbance to the robot is generally bounded. Hence, we assume that the differential of \mathbf{d} is bounded, i.e., $\sup_{t \geq 0} \|\dot{\mathbf{d}}\| \leq d_0$ for a constant $d_0 > 0$.

Theorem 1. *The disturbance estimation error $\tilde{\mathbf{d}}$ of a robot system as Eq. (8) is bounded, $\|\tilde{\mathbf{d}}(t)\| \leq \sqrt{\|\mathbf{d}(0)\|^2 e^{-t/k} + k^2 d_0^2}$, and hence the disturbance estimation $\hat{\mathbf{d}} \rightarrow \mathbf{d}$ when $k \rightarrow 0$ and/or $d_0 \rightarrow 0$.*

Proof : A Lyapunov function is designed as

$$V_1 = \frac{1}{2}\tilde{\mathbf{d}}^T \tilde{\mathbf{d}} \quad (14)$$

Then, we calculate its differential with respect to time and apply Young's inequality on $\tilde{\mathbf{d}}^T \dot{\tilde{\mathbf{d}}}$.

$$\begin{aligned} \dot{V}_1 &= \tilde{\mathbf{d}}^T \dot{\tilde{\mathbf{d}}} = -\frac{1}{k}\tilde{\mathbf{d}}^T \tilde{\mathbf{d}} + \tilde{\mathbf{d}}^T \dot{\mathbf{d}} \\ &\leq -\frac{1}{k}\tilde{\mathbf{d}}^T \tilde{\mathbf{d}} + \frac{1}{2k}\tilde{\mathbf{d}}^T \tilde{\mathbf{d}} + \frac{k}{2}d_0^2 \\ &\leq -\frac{1}{k}V_1 + \frac{k}{2}d_0^2 \end{aligned} \quad (15)$$

Thus, V_1 is proven to be bounded as well as the estimation error $\|\tilde{\mathbf{d}}(t)\|$. And $\|\tilde{\mathbf{d}}(t)\|$ will exponentially converge to a residual, $\|\tilde{\mathbf{d}}(t)\| \leq \sqrt{\|\mathbf{d}(0)\|^2 e^{-t/k} + k^2 d_0^2}$, where the bound depends on the constant k and the upper bound d_0 .

C. UDE-based Controller Design

To design a controller to track trajectory with the estimation of lumped disturbance, we define a variable

$$\mathbf{S} = \dot{\mathbf{e}} + \boldsymbol{\eta}\mathbf{e} \quad (16)$$

where $\mathbf{S} \in \mathbb{R}^n$, $\mathbf{e} = \mathbf{q} - \mathbf{q}^{des}$ is the vector of joint position error, $\boldsymbol{\eta} \in \mathbb{R}^{n \times n}$ is a positive diagonal matrix of control

coefficient. Obviously, the tracking error \mathbf{e} will converge to zero once \mathbf{S} converges to zero.

Then, we formulate the UDE-based controller as

$$\boldsymbol{\tau}^{des} = -\mathcal{K}\mathbf{S} - \hat{\mathbf{d}} + \mathbf{M}\dot{\mathbf{z}} + \mathbf{C}\mathbf{z} + \mathbf{g} \quad (17)$$

where $\mathbf{z} = \dot{\mathbf{q}}^{des} - \boldsymbol{\eta}\mathbf{e}$ is an intermediate variable, $\mathcal{K} \in \mathbb{R}^{n \times n}$ is a diagonal positive matrix of control gain, $\hat{\mathbf{d}}$ is obtained from Eq. (11). Here, \mathcal{K} keeps constant throughout the control period, while it will be designed to be time-varying in next section. Note that in the controller Eq. (17), the acceleration $\ddot{\mathbf{q}}$ is not used, nor is the inverse of the inertia matrix as in [8], since \mathbf{M}^{-1} may not be always feasible in practice according to [12]. The proof of convergence and boundedness of the proposed controller will be given in Section IV.

By substituting Eq. (17) into Eq. (3), we have the tracking error equation as

$$\mathbf{M}\dot{\mathbf{S}} = -\mathcal{K}\mathbf{S} - \mathbf{C}\mathbf{S} + \tilde{\mathbf{d}} \quad (18)$$

D. Time-varying Control Gain

According to the analysis in [18], the control gain should be selected appropriately. A too low gain will lead to low response to disturbance, while a too high gain will lead to bad damping effect. In addition, the gain value may affect the bandwidth of control system [15]. Hence, we adopt adaptive law and design time-varying control gains as Eq. (19), so that the controller can quickly adapt to complex disturbance.

$$\dot{\hat{\mathbf{x}}}_i(t) = \begin{cases} \lambda_i(s_i - \sigma_i \hat{\mathbf{x}}_i), & \text{if } \hat{\mathbf{x}}_i \geq \underline{\mathbf{x}}_i \\ 0, & \text{otherwise} \end{cases} \quad (19)$$

where $\hat{\mathbf{x}}_i$ denotes the elements on the diagonal of the estimated gain matrix $\hat{\mathcal{K}}$ as Eq. (20), and is equal to the lower bound $\underline{\mathbf{x}}_i > 0$ at initial. $\lambda_i > 0$ is the adaptive gain, s_i corresponds to the element of the vector \mathbf{S} , $\sigma_i > 0$ is a constant (i.e., σ -modification [16]). In Eq. (19), the gain $\hat{\mathbf{x}}_i$ will adaptively change as long as it is higher than $\underline{\mathbf{x}}_i$. Besides, we assume the differential of $\hat{\mathbf{x}}_i$ is bounded, i.e., $\sup_{t \geq 0} |\dot{\hat{\mathbf{x}}}_i| \leq \dot{\mathbf{x}}_{i0} < 0$ for a constant $\dot{\mathbf{x}}_{i0} > 0$.

$$\hat{\mathcal{K}} = \begin{pmatrix} \hat{\mathbf{x}}_1 & 0 & \cdots & 0 \\ 0 & \hat{\mathbf{x}}_2 & \cdots & 0 \\ \vdots & \vdots & \ddots & \vdots \\ 0 & 0 & \cdots & \hat{\mathbf{x}}_n \end{pmatrix} \quad (20)$$

Before proving the stability of Eq. (19), we give a lemma:

Lemma 2. *For the robot's i^{th} joint, the control gain $\hat{\mathbf{x}}_i$ designed by the adaptive law Eq. (19) has the following property with the estimation error $\tilde{\mathbf{x}}_i$*

$$\tilde{\mathbf{x}}_i \dot{\hat{\mathbf{x}}}_i \leq -\frac{2\gamma_1 - 1}{2\gamma_1} \tilde{\mathbf{x}}_i^2 + \frac{\gamma_1}{2} \mathbf{x}_i \quad (21)$$

where $\gamma_1 > 0$ is an arbitrary constant.

Proof : By applying Young's inequality on $\tilde{\mathbf{x}}_i \mathbf{x}_i$, we have

$$\begin{aligned} \tilde{\mathbf{x}}_i \dot{\hat{\mathbf{x}}}_i &= \tilde{\mathbf{x}}_i (\mathbf{x}_i - \hat{\mathbf{x}}_i) = -\tilde{\mathbf{x}}_i^2 + \tilde{\mathbf{x}}_i \mathbf{x}_i \\ &\leq -\tilde{\mathbf{x}}_i^2 + \frac{1}{2\gamma_1} \tilde{\mathbf{x}}_i^2 + \frac{\gamma_1}{2} \mathbf{x}_i^2 \\ &= -\frac{2\gamma_1 - 1}{2\gamma_1} \tilde{\mathbf{x}}_i^2 + \frac{\gamma_1}{2} \mathbf{x}_i^2 \end{aligned} \quad (22)$$

IV. STABILITY ANALYSIS

In this section, the convergence and boundedness of the proposed control system is proven.

Theorem 2. For a robot system Eq. (3), the closed-loop control system Eq. (17) is stable with the UDE observer Eq. (11) and the time-varying gain Eq. (19). The tracking error e , the disturbance estimation error \tilde{d} , the gain estimation error $\tilde{\kappa}$ will exponentially converge to a small residual around zero, and are all ultimately uniformly bound.

Proof : A Lyapunov function is designed as

$$V_2 = \frac{1}{2} \mathbf{S}^T \mathbf{M} \mathbf{S} + \frac{1}{2} \tilde{d}^T \tilde{d} + \frac{1}{2} \sum_{i=1}^n \frac{1}{\lambda_i} \tilde{\kappa}_i^2 \quad (23)$$

where λ_i is the adaptive coefficient defined in Eq. (19). Then, we calculate the differential of V_2 . For the convenience of proof, \dot{V}_2 is divided into two portions \mathcal{B}_1 and \mathcal{B}_2 as below.

$$\dot{V}_2 = \underbrace{\mathbf{S}^T \mathbf{M} \dot{\mathbf{S}} + \frac{1}{2} \mathbf{S}^T \dot{\mathbf{M}} \mathbf{S} + \tilde{d}^T \dot{\tilde{d}}}_{\mathcal{B}_1} + \underbrace{\sum_{i=1}^n \frac{1}{\lambda_i} \tilde{\kappa}_i \dot{\tilde{\kappa}}_i}_{\mathcal{B}_2} \quad (24)$$

For \mathcal{B}_1 , substitute Eq. (12), Eq. (18), and apply Young's inequality on $\mathbf{S}^T \tilde{d}$ and $\tilde{d} \dot{\tilde{d}}$ as

$$\begin{aligned} \mathcal{B}_1 &= \mathbf{S}^T (-\mathcal{K} \mathbf{S} - \mathbf{C} \mathbf{S} + \tilde{d}) + \frac{1}{2} \mathbf{S}^T \dot{\mathbf{M}} \mathbf{S} + \tilde{d}^T (-\frac{1}{k} \tilde{d} + \dot{d}) \\ &= -\mathbf{S}^T \mathcal{K} \mathbf{S} + \mathbf{S}^T \tilde{d} - \frac{1}{k} \tilde{d}^T \tilde{d} + \tilde{d} \dot{\tilde{d}} \\ &\leq -\gamma_2 \mathbf{S}^T \mathbf{S} + (\frac{\gamma_2}{2} \mathbf{S}^T \mathbf{S} + \frac{1}{2\gamma_2} \mathbf{d}^T \mathbf{d}) - \frac{1}{k} \tilde{d}^T \tilde{d} \\ &\quad + (\frac{1}{2k} \tilde{d}^T \tilde{d} + \frac{k}{2} d_0^2) \\ &= -\frac{\gamma_2}{2} \mathbf{S}^T \mathbf{S} - (\frac{1}{2k} - \frac{1}{2\gamma_2}) \tilde{d}^T \tilde{d} + \frac{k}{2} d_0^2 \end{aligned} \quad (25)$$

where $\gamma_2 = \lambda_{min}(\mathcal{K})$ is the minimum eigenvalue of \mathcal{K} , d_0 is the upper bound of differential of disturbance $\|\dot{d}\|$.

For \mathcal{B}_2 , substitute Eq. (19), Eq. (21), and apply Young's inequality on $\tilde{\kappa}_i \dot{\tilde{\kappa}}_i$ and $-\tilde{\kappa}_i s_i$ as

$$\begin{aligned} \mathcal{B}_2 &= \sum_{i=1}^n \frac{1}{\lambda_i} \tilde{\kappa}_i (\dot{\tilde{\kappa}}_i - \tilde{\kappa}_i) = \sum_{i=1}^n \frac{1}{\lambda_i} \tilde{\kappa}_i \dot{\tilde{\kappa}}_i - \sum_{i=1}^n \tilde{\kappa}_i (s_i - \sigma_i \hat{\kappa}_i) \\ &\leq \sum_{i=1}^n \frac{1}{\lambda_i} (\frac{1}{2\gamma_3} \tilde{\kappa}_i^2 + \frac{\gamma_3}{2} \dot{\tilde{\kappa}}_i^2) + \sum_{i=1}^n (\frac{1}{2\gamma_4} \tilde{\kappa}_i^2 + \frac{\gamma_4}{2} s_i^2) \\ &\quad + \sum_{i=1}^n \sigma_i (-\frac{2\gamma_1 - 1}{2\gamma_1} \tilde{\kappa}_i^2 + \frac{\gamma_1}{2} \dot{\tilde{\kappa}}_i^2) \\ &\leq -\sum_{i=1}^n \frac{1}{2} \underbrace{\left[\frac{(2\gamma_1 - 1)\sigma_i}{\gamma_1} - \frac{1}{\lambda_i \gamma_3} - \frac{1}{\gamma_4} \right]}_{\mathcal{E}} \tilde{\kappa}_i^2 \\ &\quad + \underbrace{\sum_{i=1}^n (\frac{\gamma_3}{2\lambda_i} \tilde{\kappa}_{i0}^2 + \frac{\gamma_1 \sigma_i}{2} \dot{\tilde{\kappa}}_i^2)}_{\mathcal{F}} + \sum_{i=1}^n \frac{\gamma_4}{2} s_i^2 \\ &= \frac{\gamma_4}{2} \mathbf{S}^T \mathbf{S} - \sum_{i=1}^n \frac{\mathcal{E}}{2} \tilde{\kappa}_i^2 + \mathcal{F} \end{aligned} \quad (26)$$

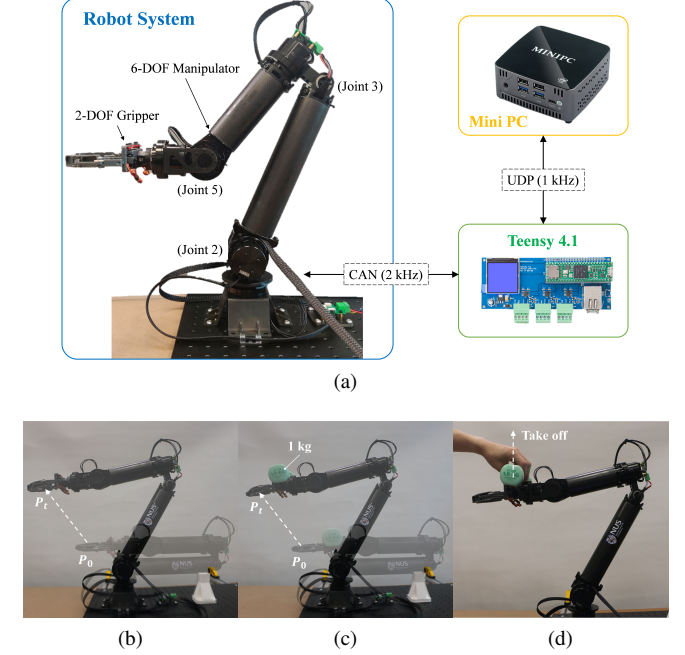


Fig. 2. Experimental setup. (a) shows a robotic manipulator and accompanying electronics. The bottom pictures are snapshots of three groups of experiments, which correspond to (b) free-motion tracking, (c) static-disturbance tracking, and (d) dynamic-disturbance test, respectively.

where $\gamma_3, \gamma_4 > 0$ are arbitrary constants. $\tilde{\kappa}_{i0}$ is the upper bound of differential of control gain $\dot{\tilde{\kappa}}_i$. \mathcal{E} and \mathcal{F} are intermediate variables for the convenience of proof.

Hence, combining Eq. (25) and Eq. (26), we have

$$\begin{aligned} \dot{V}_2 &\leq -\frac{\gamma_2 - \gamma_4}{2} \mathbf{S}^T \mathbf{S} - (\frac{1}{2k} - \frac{1}{2\gamma_2}) \tilde{d}^T \tilde{d} - \sum_{i=1}^n \frac{\mathcal{E}}{2} \tilde{\kappa}_i^2 \\ &\quad + (\frac{k}{2} d_0^2 + \mathcal{F}) \\ &\leq -\alpha V_2 + \beta \end{aligned} \quad (27)$$

with

$$\alpha = \min \left\{ \frac{\gamma_2 - \gamma_4}{\lambda_{max}(\mathbf{M})}, (\frac{1}{k} - \frac{1}{\gamma_2}), \lambda_i \mathcal{E} \right\} \quad (28)$$

$$\beta = \frac{k}{2} d_0^2 + \mathcal{F} = \frac{k}{2} d_0^2 + \sum_{i=1}^n (\frac{\gamma_3}{2\lambda_i} \tilde{\kappa}_{i0}^2 + \frac{\gamma_1 \sigma_i}{2} \dot{\tilde{\kappa}}_i^2) \quad (29)$$

where $\lambda_{max}(\mathbf{M})$ is the maximum eigenvalue of \mathbf{M} . β is a positive constant, while we set constraints as below to make the constant $\alpha > 0$ as well.

$$\begin{cases} \gamma_2 \geq \gamma_4 \\ \gamma_2 \geq k \\ \sigma_i \geq \frac{(\lambda_i \gamma_3 + \gamma_4) \gamma_1}{\lambda_i \gamma_3 \gamma_4 (2\gamma_1 - 1)} \end{cases} \quad (30)$$

Finally, by solving Eq. (27), we have $V_2(t) \leq e^{-\alpha t} V_2(0) + \beta/\alpha(1 - e^{-\alpha t})$. Therefore, Theorem 2 is proven.

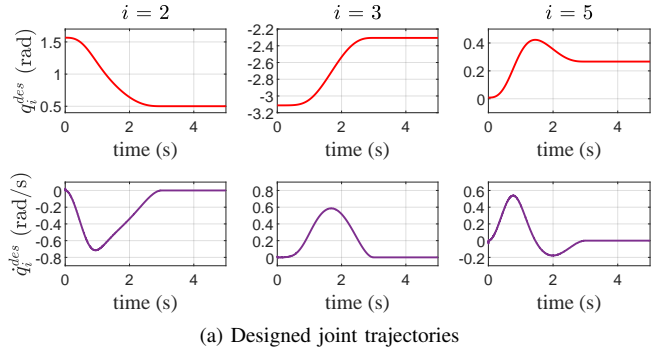
V. VERIFICATION

The experimental verification is conducted on a six-DOF robotic manipulator with a two-DOF gripper, depicted in Fig. 2(a), which is developed by NUS Biorobotics Laboratory. The robot system weighs approximately 4 kg and is capable of taking a maximum payload of 1 kg at full extension of 600 mm. Each joint consists of a torque-controlled BLDC motor and a harmonic drive with reduction ratio of 50. The motors are connected to a low-level controller Teensy 4.1 via CAN at 2 kHz, and the latter communicates with a Mini PC (Intel Core i7-1165G7 CPU, Linux kernel 5.4.69-rt39) via UDP at 1 kHz. The C++ implementation of our control algorithm can run at a frequency of 500 Hz on the PC.

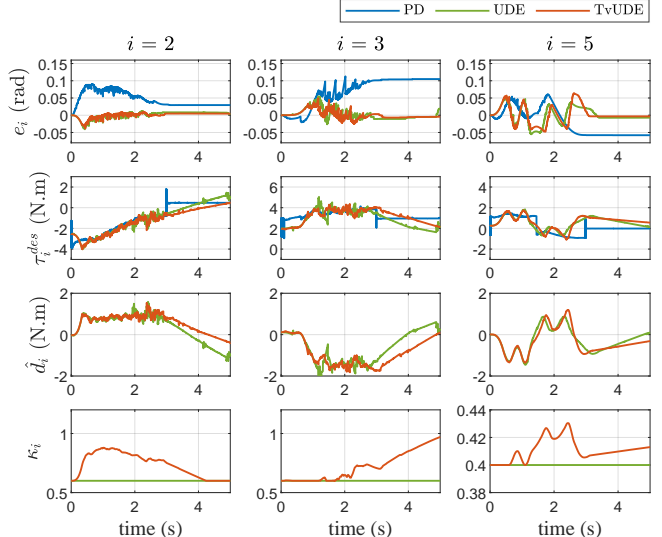
To demonstrate the effectiveness of the proposed TvUDE controller, we compare it to the other two controllers, i.e., an UDE controller as Eq. (17) but with constant control gains, and a PD feedback controller plus model-based feedforward [17]. Correspondingly, we carry out comparison experiments that are divided into three groups in total. First, the manipulator is required to freely track a straight trajectory from P_0 to P_t in Cartesian space, as illustrated in Fig. 2(b). The second group uses a 1 kg dumbbell as an unmodeled static disturbance in the tracking stage, as Fig. 2(c) shown. For the third group in Fig. 2(d), the 1 kg dumbbell is immediately removed from the robot as it is keeping position to simulate transient disturbance.

The control parameters are kept consistent in the three test cases. Here we only discuss the results of joint 2, joint 3 and joint 5 (i.e., $i = 2, 3, 5$) due to their obvious effect. For the PD controller, the proportional gain is (5, 5, 5); the differential gain is (0.5, 0.5, 0.5); the Coulomb friction compensation is roughly identified as (1.3, 0.9, 0.9) N.m. Then, for the UDE controller, the filter gain $k = 0.05$; the tracking error gain η_i is (10, 10, 10) while the constant control gain \varkappa_i is (0.6, 0.6, 0.4). Moreover, the adaptive gain λ_i in the TvUDE controller is (2.5, 2.5, 0.1); the lower bound $\underline{\varkappa}_i$ for activating adaption keeps same as \varkappa_i of the UDE.

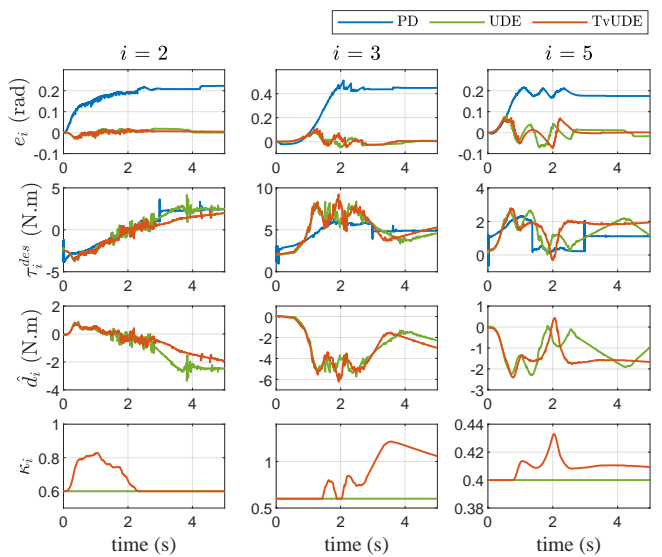
Fig. 3 provides the recorded command and measurement in free-motion and static-disturbance tests. Fig. 3 (a) indicates the joint position q_i^{des} and velocity \dot{q}_i^{des} command computed by the IK solver Eq. 2 that allows the end-effector to follow a straight line. In Fig. 3 (b) and Fig. 3 (c), from the top row to the bottom, they are the tracking error e_i , the commanded joint torque τ_i^{des} , the estimation of lumped disturbance \hat{d}_i , and the control gain \varkappa_i . The robot joints start moving in 0-3 seconds, and then stop when the end-effector reaches the targeted location. Both tests present excellent tracking performance of the controllers with estimation, compared to the pure PD. For example, in Fig. 3(b), the blue curve representing the PD shows a slightly large transient tracking error as well as steady-state error, probably due to inaccurate friction model. However, even without friction compensation, the UDE (green curve) and the TvUDE (red curve) only lead to small tracking error. The disturbance \hat{d}_i estimated online also reflects that the friction in real world is too complex to be modelled exactly. Furthermore, after adding unknown



(a) Designed joint trajectories



(b) Free-motion tracking



(c) Static-disturbance tracking

Fig. 3. Plots showing the recorded command and measurement in free-motion and static-disturbance tests. (a) shows the joint position q_i^{des} and velocity \dot{q}_i^{des} command computed by the IK solver. In (b) and (c), from the top row to the bottom, they are the tracking error e_i , the commanded joint torque τ_i^{des} , the estimated lumped disturbance \hat{d}_i , and the control gain \varkappa_i .

payload on the robot, the PD behaves worse while the two controllers with UDE can still handle model uncertainty as

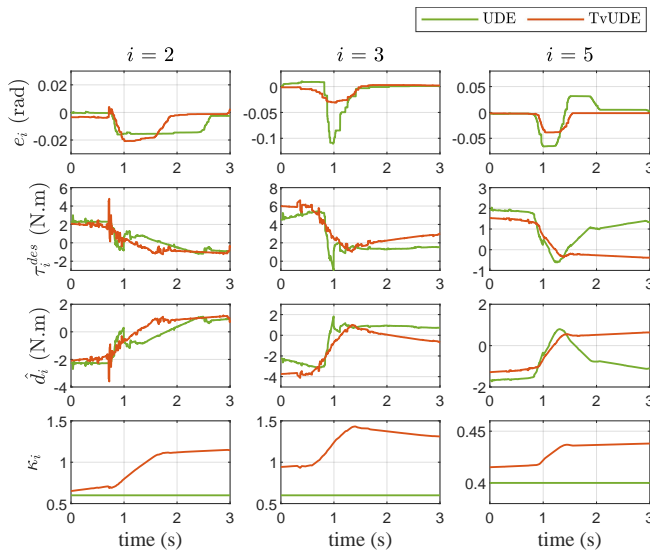


Fig. 4. Experimental results in transient-disturbance test. Similarly, e_i , τ_i^{des} , d_i , and ξ_i of the two controllers with UDE are recorded.

well as external disturbance with very small tracking errors, as illustrated in Figure 3(c). Note that the gain ξ_i continuously changes, indicating that the adaptive law functions all the time, though there appears to be no improvement in tracking. The time-varying gain does however help the controller continue to work well under transient disturbance.

The result in Fig. 4 corresponds to the third group of experiments, which compares the UDE and the TvUDE on dealing with transient disturbance. In this case, when the dumbbell is taken off at 0.8 seconds, all joints oscillate to some degree, and then return back to their previous position. However, the TvUDE controller presents shorter recovery time and less tracking error than the UDE. The faster convergence rate of TvUDE can be explained from the control gain ξ_i plots. When disturbance occurs, the control gain (red curve) rapidly increases to stabilize the robot as soon as possible. Therefore, the TvUDE shows strong robustness to reject transient disturbance. More experiment results can be found in our video submission.

VI. CONCLUSION AND FUTURE WORK

In this paper, we propose an efficient and robust motion controller (TvUDE) with uncertainty and disturbance estimation and time-varying control gain for robotic manipulators, in order to achieve precise trajectory tracking. Specifically, the estimator that consists of reformulated robot dynamics and filtering operations can estimate unknown disturbance in real time, without using the acceleration signal. Then, the time-varying control gain based on the gradient method intends to further increase the robustness of the control system. Finally, the convergence performance and boundness of TvUDE is analysed, while a set of real hardware experiments are conducted on a six-DOF robotic manipulator for verification. The experimental results show the effectiveness of the proposed controller on handling internal uncertainty, external static and transient disturbance. In the future, we

plan to study the possibility of this controller in collision detection for safe human-robot collaboration.

ACKNOWLEDGMENT

The authors are grateful to Terry Cavan Chan for his help in mechanical design of the robot.

REFERENCES

- [1] A. Billard and D. Kragic, “Trends and challenges in robot manipulation,” *Science*, vol. 364, no. 6446, p. eaat8414, 2019.
- [2] L. Márton and B. Lantos, “Control of mechanical systems with stieber friction and backlash,” *Systems & Control Letters*, vol. 58, no. 2, pp. 141–147, 2009.
- [3] J. J. Craig, *Introduction to Robotics: Mechanics and Control*. Pearson Prentice Hall, 2005.
- [4] J. Swevers, W. Verdonck, and J. De Schutter, “Dynamic model identification for industrial robots,” *IEEE Control Systems Magazine*, vol. 27, no. 5, pp. 58–71, 2007.
- [5] K. Lu, Z. Liu, C. P. Chen, Y. Wang, and Y. Zhang, “Inverse optimal design of direct adaptive fuzzy controllers for uncertain nonlinear systems,” *IEEE Transactions on Fuzzy Systems*, vol. 30, no. 6, pp. 1669–1682, 2021.
- [6] W.-H. Chen, J. Yang, L. Guo, and S. Li, “Disturbance-observer-based control and related methods—an overview,” *IEEE Transactions on Industrial Electronics*, vol. 63, no. 2, pp. 1083–1095, 2016.
- [7] K. Ohishi, M. Nakao, K. Ohnishi, and K. Miyachi, “Microprocessor-controlled dc motor for load-insensitive position servo system,” *IEEE Transactions on Industrial Electronics*, vol. IE-34, no. 1, pp. 44–49, 1987.
- [8] W.-H. Chen, D. Ballance, P. Gauthrop, and J. O'Reilly, “A nonlinear disturbance observer for robotic manipulators,” *IEEE Transactions on Industrial Electronics*, vol. 47, no. 4, pp. 932–938, 2000.
- [9] J. Han, “From pid to active disturbance rejection control,” *IEEE Transactions on Industrial Electronics*, vol. 56, no. 3, pp. 900–906, 2009.
- [10] W. Xue, W. Bai, S. Yang, K. Song, Y. Huang, and H. Xie, “Adrc with adaptive extended state observer and its application to air-fuel ratio control in gasoline engines,” *IEEE Transactions on Industrial Electronics*, vol. 62, no. 9, pp. 5847–5857, 2015.
- [11] S. Lu, C. Tian, and P. Yan, “Adaptive extended state observer-based synergetic control for a long-stroke compliant microstage with stress stiffening,” *IEEE/ASME Transactions on Mechatronics*, vol. 25, no. 1, pp. 259–270, 2020.
- [12] J. Na, B. Jing, Y. Huang, G. Gao, and C. Zhang, “Unknown system dynamics estimator for motion control of nonlinear robotic systems,” *IEEE Transactions on Industrial Electronics*, vol. 67, no. 5, pp. 3850–3859, 2020.
- [13] J. Na, J. Yang, S. Wang, G. Gao, and C. Yang, “Unknown dynamics estimator-based output-feedback control for nonlinear pure-feedback systems,” *IEEE Transactions on Systems, Man, and Cybernetics: Systems*, vol. 51, no. 6, pp. 3832–3843, 2021.
- [14] J. Yang, J. Na, H. Yu, G. Gao, and X. Wang, “Unknown system dynamics estimator for nonlinear uncertain systems,” in *2020 International Federation of Automatic Control (IFAC)*, vol. 53, no. 2, 2020, pp. 554–559.
- [15] S. Han, H. Wang, Y. Tian, and H. Yu, “Enhanced extended state observer-based model-free force control for a series elastic actuator,” *Mechanical Systems and Signal Processing*, vol. 183, p. 109584, 2023.
- [16] P. A. Ioannou and J. Sun, *Robust Adaptive Control*. Courier Corporation, 2012.
- [17] K. Lynch and F. Park, *Modern Robotics: Mechanics, Planning, and Control*. Cambridge University Press, 2017.
- [18] M. Ezzeldin, P. van den Bosch, and R. Waarsing, “Improved convergence of mrac design for printing system,” in *2009 American Control Conference (ACC)*, 2009, pp. 3232–3237.